Laser and Particle Beams (2004), *22*, 207–213. Printed in the USA.

DOI: 10.1017/S0263034604223035

Tracking ground state Ba^+ ions in an expanding laser–plasma plume using time-resolved vacuum ultraviolet photoionization imaging

J.S. HIRSCH,[1] K.D. KAVANAGH,[1] E.T. KENNEDY,[1] J.T. COSTELLO,[1] P. NICOLOSI,[2] AND L. POLETTO[2]

[1]National Centre for Plasma Science and Technology (NCPST) and School of Physical Sciences, Dublin City University, Dublin 9, Ireland
[2]Istituto Nazionale per la Fisica della Materia, Universita di Padova, Via Granenigo, Padova, Italia

(RECEIVED 1 November 2003; ACCEPTED 17 February 2004)

Abstract

We report results from a study of the integrated column density and expansion dynamics of ground-state-selected Ba^+ ions in a laser–plasma plume using a new experimental system—VPIF (vacuum-ultraviolet photoabsorption imaging facility). The ions are tracked by recording the attenuation of a pulsed and collimated vacuum ultraviolet beam, tuned to the $5p$–$6d$ inner-shell resonance of singly ionized barium, as the expanding plasma plume moves across it. The attenuated beam is allowed to fall on a CCD array where the spatial distribution of the absorption is recorded. Time-resolved ion velocity and integrated column density maps are readily extracted from the photoionization images.

Keywords: Barium; Imaging; Laser plasma; Photoabsorption; Vacuum ultraviolet

1. INTRODUCTION

Photoabsorption imaging using tuneable optical lasers is a well-established technique for tracking the evolution of dilute and nonemitting dynamic samples. For example, it can be used to measure the evolution of momentum distributions in expanding atomic Bose–Einstein condensates (Hecker-Denschlag *et al*., 2002). It has also been used successfully to measure late phase absorption in laser plasma plumes (Williamson *et al*., 1999). However, for more dense samples (e.g., laser–plasma plumes in the early stages of formation and growth) the analysis of absorption signals can be complicated by the need to invoke the full radiative transfer equation. Moving to the vacuum ultraviolet (VUV) spectral range, where one can excite inner-shell and multiply excited resonances, which decay predominantly by autoionization, greatly relaxes this restriction. In fact, in most cases the probability for autoionization dominates over that for photon emission (fluorescence) and one can readily rely on a simple Beer–Lambert prescription to describe the beam attenuation. The measurement made (total photoabsorption) is then also, in effect, a measure of the total photoionization signal and hence the technique can legitimately be termed "photoionization imaging."

Probing plasma plumes with VUV light has a number of other advantages over optical probing, including the ability to access the resonance lines of ions, which usually lie in the VUV. In addition, refraction of the VUV probe beam by the plume density gradient, which typically scales as λ^2_{probe} (Attwood *et al*., 1975), is reduced. Because the VUV beam has a coherence length of typically less than a few microns (Turcu *et al*., 1993), absorption images are free from the interference effects observed on images obtained in laser absorption experiments. Finally the absorption image data, representing as they do the dark or nonemitting species in the plume, complement the usual optically filtered and gated emission images that provide insights only into the spatial distribution of excited state plasma species (Geohegan, 1993).

We demonstrated some time ago the proof of principle and application of photoabsorption imaging as a plasma plume diagnostic (Hirsch *et al*., 2000). Encouraged by those positive results we designed and have just completed the construction and characterization of a new experimental

Address correspondence and reprint requests to: John T. Costello, National Centre for Plasma Science and Technology (NCPST) and School of Physical Sciences, Dublin City University, Dublin 9, Ireland. E-mail: john.costello@dcu.ie

facility called VPIF (vacuum-ultraviolet photoabsorption imaging facility) to fully exploit the potential of this novel diagnostic (Hirsch *et al*., 2003). We report here some early results from a study of the ion-integrated column density and expansion dynamics of ground-state-selected Ba^+ ions in a laser–plasma plume using the VPIF. We chose singly ionized barium to showcase the technique because its VUV photoion spectrum is now well known, with resonance positions and absolute photoionization cross sections available (Lyon *et al*., 1986). These measured data facilitate the extraction of integrated column densities $[NL = \int n(l)dl]$ directly from the photoabsorption images (see below). In addition, the VUV absorption spectra of atomic Ba (Rose *et al*., 1980) and Ba^{2+} (Hill *et al*., 1982) have also been measured and their complex structure unravelled so that transitions with excitation energies unique to Ba^+ may be isolated to ensure photoabsorption images are free from contamination by neighboring charge states in the plasma plume. The aforementioned isolated resonances of Ba^+ have peak cross sections that ensure that the VUV absorption is not saturated at the high end of the integrated column density scale (shortly after Ba plasma ignition) while providing good absorption during the expansion phase up to a few hundred nanoseconds after breakdown. Barium is also a component of the High T_c superconductor yttrium barium copper oxide (YBCO) and data on the expansion of the individual atomic components in an expanding plasma plume would be valuable for comparison with the multi-element YBCO plasma and of interest to the relevant laser-deposited thin superconducting film community (Reade *et al*., 1992). Finally barium, released at high altitude, forms plasma clouds that are used to probe space weather conditions (Horwitz & Moore, 2000). It is known that these lowly ionized Ba plasma clouds move rapidly, typically 1–10 km/s (Wescott *et al*., 1993) and hence an expanding laser-produced Ba plasma plume could make for an interesting and potentially useful comparative model system.

2. EXPERIMENT

A schematic diagram of the setup is shown in Figure 1. It produces a pulsed, collimated, and wavelength-tuneable VUV (30–100 nm) beam of approximately square cross section of 4 mm on each side that can be passed through a dynamic (or static) sample and the attenuation recorded on a VUV sensitive charge-coupled device (CCD). Here the continuum backlight was a laser-produced gold plasma that provided VUV pulses of ca. 20 ns duration at a repetition rate of 10 Hz. This "source" plasma was formed by focusing the 800-mJ/8-ns/1064-nm output from a Continuum Surelite laser to a spot size of <60 μm onto a gold rod. Radiation from the source plasma was focused by an optimized toriodal mirror onto the entrance slit of an Acton Research Corp. VM521 vacuum monochromator. The exit beam was then collimated by a second toroid before being directed through the expanding Ba plasma plume. Using 50-μm/50-μm exit/entrance slits, we obtained a resolving power ($\lambda/\Delta\lambda$) of >1000 at a wavelength of 50 nm.

The Ba "sample" plasma was formed by focusing the 300-mJ/15-ns/1064-nm output from a Spectron SL404G laser onto a Ba slab to a line some 3 mm long and 100 μm high using a cylindrical lens. The barium plasma was occluded from the direct view of the CCD by retracting the Ba slab until its surface lay some 0.50 mm behind a knife edge. The parallel VUV beam just clipped the knife edge and so the VUV beam passed 0.5 mm above the target surface. The effect was to reduce significantly the unwanted radiation from Ba plasma that fell on the CCD. In addition we placed a thin (200 nm thick) aluminum foil between the Ba target and CCD to further reduce unwanted UV and visible emission from the expanding (Ba) plume that extended beyond the knife edge and is probed by the CCD.

The Ba^+ ions were tracked by recording the time-resolved attenuation of the pulsed VUV beam, tuned to the 46.7-nm inner-shell resonance array of singly ionized bar-

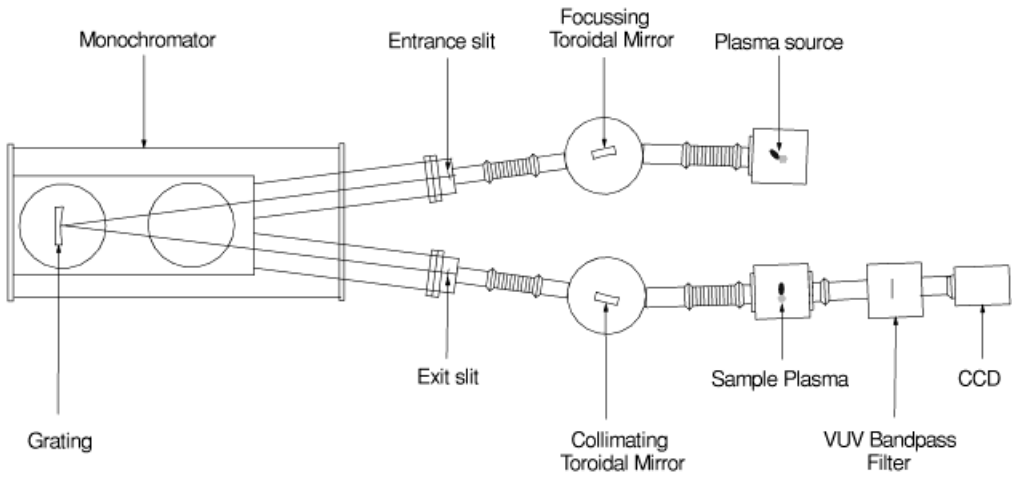

Fig. 1. Schematic diagram of the vacuum-UV photoabsorption facility (VPIF).

ium as the expanding plasma plume moved through it. This feature (as yet unclassified but tentatively assigned as a $5p-6d$ array) is well isolated from any nearby resonant structure in Ba and Ba^{2+}. The attenuated beam was allowed to fall on the CCD array where the spatial distribution of the absorption signal $\int I_\lambda(L)d\lambda$ was recorded by firing the continuum source laser at a delay $\Delta\tau$ after the barium plasma breakdown. Here, $\int I_\lambda(L)d\lambda$ is the VUV flux transmitted through a sample of length L, contained within the monochromator bandwidth ($\Delta\lambda$) and integrated by the CCD array over the ca. 20-ns VUV pulse duration.

These measured values can be related directly to the equivalent width W_λ for a plasma length L, following the equation

$$W_\lambda = \Delta\lambda \times \left(\frac{\int_{\Delta\lambda} [I_\lambda(0) - I_\lambda(L)]d\lambda}{\int_{\Delta\lambda} I_\lambda(0)d\lambda} \right), \qquad (1)$$

where $\int I_\lambda(0)d\lambda$ is the unattenuated VUV flux, contained within the monochromator bandwidth ($\Delta\lambda$) and integrated by the CCD array over VUV pulse width.

3. RESULTS AND BRIEF DISCUSSION

In Figure 2 we show time-resolved maps of equivalent width (W_λ) for Ba^+ recorded on the 46.7-nm, $5p-6d$ resonance for various delays $\Delta\tau$ in the range 100–700 ns. The effective pixel size in each image is 78×78 μm^2 because we bin 6×6 (13×13 μm^2) CCD pixels to improve image signal-to-noise ratio. The continuum beam bandwidth was 0.1 nm using 100-μm/100-μm entrance/exit slit widths. The focused laser beam is coming from the left-hand side and forms a horizontal line plasma on the Ba surface. The images show clearly how the Ba^+ plasma (ground state) component appears from behind the knife edge (which provides the sharp defining edge on the right-hand side of each image) at early times. It expands differentially along the target normal and lateral directions to form initially semi-elliptical plumes (at least in the vertical plane imaged here). At later times the plasma appears to decouple itself from the target surface to form a ball-like plume before dissipating. This phase of the expansion into vacuum is difficult to observe in gated emission images of plasma plumes. The main reason is that the density of emitting species tends to drop below the detection threshold of intensified CCD cameras at long time delays (Neogi & Thareja, 1999). Because photoabsorption cross sections for atoms and ions are highest in the VUV, we should be able to better track the "end-of-life" phase of plume expansion using the VPIF.

For a continuum source with a flat intensity distribution over the beam bandwidth $\Delta\lambda$ one can show that the equivalent width distribution for an absorbing plasma column of length L may be written as

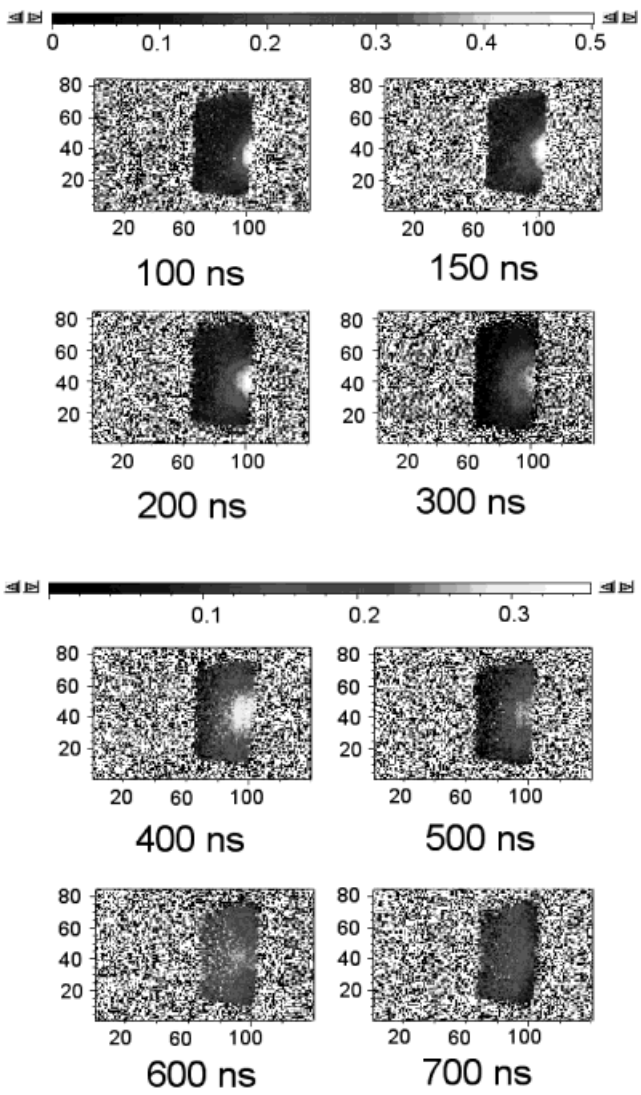

Fig. 2. Time-resolved (equivalent width) maps of the Ba^+ (46.7 nm) resonance. The bandwidth of the VUV probe beam was 0.1 nm.

$$W_\lambda = \Delta\lambda \times \left(\frac{\int_{\Delta\lambda} [I_\lambda(0) - I_\lambda(L)]d\lambda}{\int_{\Delta\lambda} I_\lambda(0)d\lambda} \right)$$

$$= \int_{\Delta\lambda} (1 - e^{-NL\int_{\Delta\lambda}\sigma_\lambda d\lambda})d\lambda, \qquad (2)$$

where N is the species density (in cm^{-3}), L is the absorbing plasma column length, and σ_λ is the absolute cross section profile. Because the absolute cross section for the transition array in the 46.7 nm region is known (Lyon *et al.*, 1986) we have been able to convert maps of equivalent width (Fig. 2)

into corresponding Ba^+ integrated column density maps using Eq. (2) and the following procedure. Briefly we generate a table of values of equivalent width W_λ for a range of NL values and construct a plot of NL versus W_λ. We then make a fit to the $NL(W_\lambda)$ curve that may be used to convert, with a simple MATLAB routine, each equivalent width pixel value into a corresponding integrated column density value. In Figure 3 we show a sequence of such integrated column maps for time delays spanning 100–500 ns following barium plasma breakdown. At these time delays, and for the on-target irradiance used, we know from our studies of Ba and La plasmas in dual laser plasma spectroscopy experiments (Köble *et al.*, 1995) that the plasma is composed predominantly of a mixture of atomic and singly ionized barium. The gray scale covers the observed range of column density, approximately 5×10^{14} cm^{-2} to 4×10^{15} cm^{-2}. The

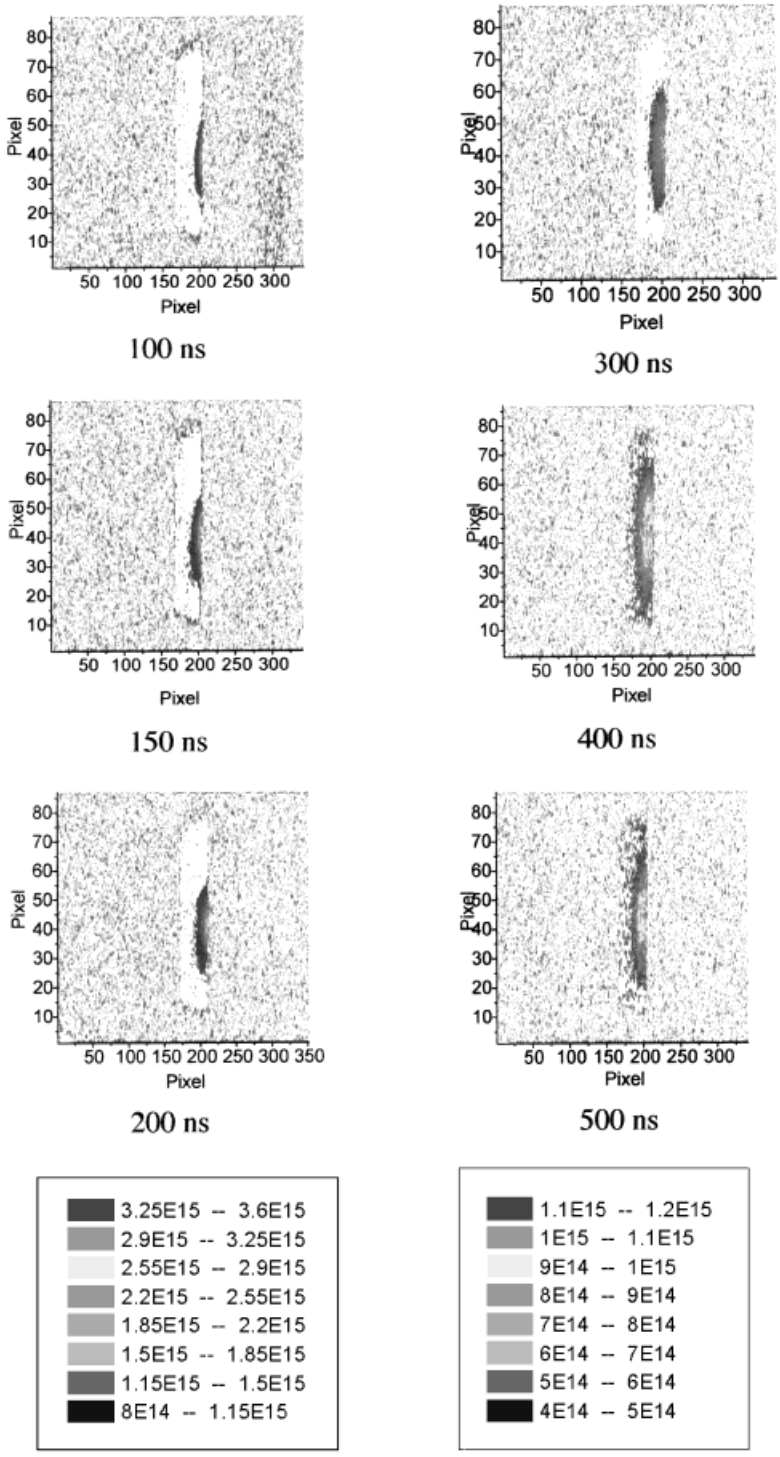

Fig. 3. Spatial distributions of integrated column density extracted from the maps of equivalent width for the 46.7-nm resonance at interlaser delays in the 100–500-ns range.

upper limit is set by the need to avoid saturated absorption and the lower limit by the noise floor in the images. We are currently working to improve the dynamic range by improving the source flux (Murphy *et al.*, 2003), reducing the detector noise floor and also reducing further the residual background emission that falls on the CCD detector.

In Figure 4 we demonstrate the tunability of the technique by showing maps of equivalent width for various wavelength detunings from the 46.7 nm resonance peak. The data were taken at a time delay $\Delta\tau$ of 200 ns using 50-μm/50-μm entrance/exit slits, giving a VUV probe bandwidth of 0.05 nm. The asymmetry in the image densities is simply a reflection of the complex and asymmetric shape of the resonance structure itself (see Fig. 4, top panel). For cases where integrated column densities $NL = \int n(l)dl$ are so high as to cause saturation (and where, simultaneously, weaker resonances free from overlap with transitions from neighboring ion stages are not available), such off-resonance detuning should prove to be an effective solution.

To simulate the plasma expansion dynamics, or, more particularly, the plasma plume expansion velocity, we have used a rather simple model (Singh & Narayan, 1990). This model distinguishes three phases in the laser-plasma life cycle: the laser interaction with the target material, the laser interaction with the evaporated material, and finally adiabatic expansion in vacuum after termination of the laser pulse. Here we are only concerned with the last phase because all measurements are made after termination of the laser pulse. The equation describing the expansion is

$$X(t)\left(\frac{d^2X}{dt^2}\right) = Y(t)\left(\frac{d^2Y}{dt^2}\right) = Z(t)\left(\frac{d^2Z}{dt^2}\right) = \frac{kT_0}{M}\left(\frac{X_0Y_0Z_0}{X(t)Y(t)Z(t)}\right)^{\gamma-1}, \quad (3)$$

where X_0, Y_0, and Z_0 are the initial plasma dimensions at the end of the laser pulse, $X(t)$, $Y(t)$, and $Z(t)$ are the dimensions of the plasma, T_0 is the temperature at the end of the laser pulse, M is the atomic mass, and γ is the specific heat capacity ratio. Equation (3) shows that the plasma expansion depends on the initial dimensions of the plasma plume, the initial temperature, and the atomic mass of the species considered. In Figure 5 we compare the size of the measured plasma plume in the direction of the laser pulse with the simulated dimensions from the expansion code. The results were obtained for an initial temperature of 10 eV and initial plasma dimensions of length 3 mm and width 0.1 mm. The initial plasma temperature of 10 eV was computed using Eq. (22) of Colombant and Tonon (1973) for our laser wavelength (1064 nm) and on target irradiance of $\sim$7 GW$\cdot$cm^{-2}.

The plasma plume dimensions were obtained by taking as a reference point the position at which the absorption signal dropped by 50% and following this point with time. Although the measured values lie above the computed curve (Fig. 5),

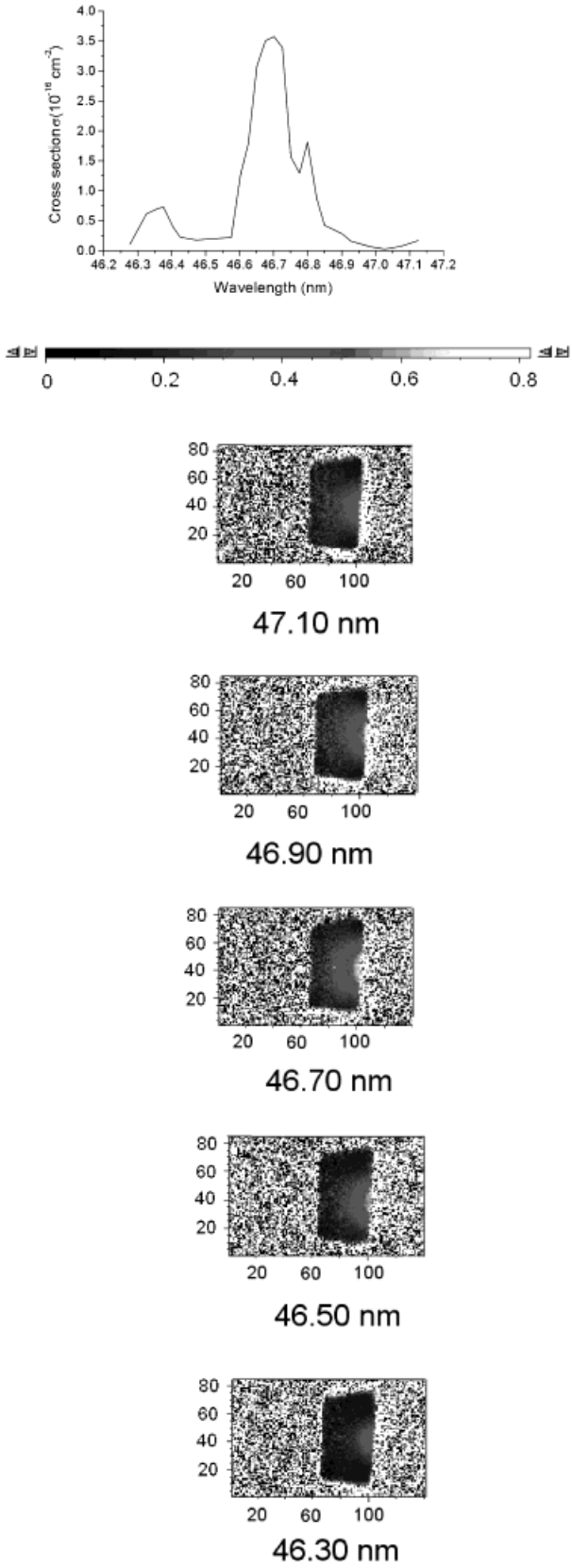

Fig. 4. Maps of equivalent width recorded at different wavelength settings and at an interlaser delay of 200 ns. Insert: the absolute photoionization cross section of Ba^+ (Lyon *et al.*, 1986). The bandwidth of the VUV probe beam was 0.05 nm.

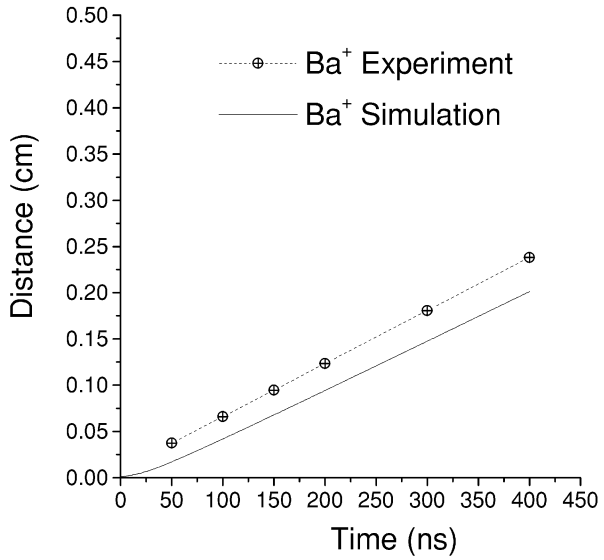

Fig. 5. Comparison between the measured front plasma plume velocity and the calculated velocity using the laser–plasma plume expansion model of Singh and Narayan (1990).

we observe the same linear increase in the plasma dimension with time. Both lines have similar slopes and the velocity of 5.7×10^5 cm s^{-1} measured experimentally compares well with the simulated value of 5.9×10^5 cm s^{-1}. However, it must be emphasized that the measured images are both charge and electronic state selective and the model used concerns the whole plume expansion. Hence it is rather fortuitous that they agree so well and is most likely a reflection that the plume is predominantly composed of Ba^+ at the times probed here. The result points to a need for more sophisticated simulations, encompassing hydrodynamics, kinetics, and atomic physics in an (ideally) self-consistent single simulation (or at least in a sequential postprocessing fashion) for the low temperature plasma plumes of currently significant interest to the pulsed laser deposition community.

4. SUMMARY

We have demonstrated the use of a vacuum-UV photoabsorption facility providing a pulsed, wavelength-tuneable, and collimated VUV beam to probe the expansion dynamics of Ba^+ in an expanding Ba plasma plume. Time-resolved equivalent width and integrated column density (NL) maps of single ionized barium after the termination of the plasma-producing laser pulse have been extracted and presented. NL for Ba^+ drops by an order of magnitude or so over the time period sampled here of 100 ns–500 ns and an expansion velocity of $5.7 \pm 0.5 \times 10^5$ cm$\cdot s^{-1}$.

Although only a small number of measured absolute photoionization cross sections (including resonances) were available in the literature until recently, a number of new experiments based on merged ion and synchrotron beams at, for example, the Advanced Light Source (ALS) in Berkeley and at the ASTRID storage ring in Aarhus are already producing copious absolute data (West, 2002). Hence the applicability of resonant photoionization imaging is set to widen to many other ion species over the coming years. Future applications that involve probing the interaction region of two colliding plasmas or of a plasma with a surface are planned. For the case of two interpenetrating plasmas, we should be able to effectively perform novel atomic collisions type experiments with full space and time resolution. Because we have charge and state of excitation selectivity, permitting us to track the depletion (and even the filling) of ion electronic states during the interaction, we will obtain fuller information than that obtained in traditional beam–beam collisions. Although experiments on imaging the fragments from collision events are now appearing (Schultz *et al.*, 2003), to our knowledge such experiments have not been performed in the past even with traditional ion beams, much less with more practical cases like plasmas. We will also combine ICCD emission imaging and spectroscopy with photoabsorption imaging to correlate our absorption with emission data (e.g., Geohegan 1993) already available in the literature for low temperature PLD plumes.

ACKNOWLEDGMENTS

We are grateful to Dr. Jean Paul Mosnier for a number of useful discussions during the course of this work and to Dr. Wil Whitty for the use of a code based on the Singh and Narynan (1990) plume expansion model. Kevin Kavanagh acknowledges scholarship funding from the Irish Research Council for Science, Engineering and Technology (IRCSET). John Hirsch is funded by the EU under contract no. HPRI-CT-1999-50099. Work supported by Irish Government National Development Plan including the HEA-PRTLI Scheme and the Basic Research Grants Scheme as administered by SFI, IRCSET and Enterprise Irland.

REFERENCES

Attwood, D.T., Coleman L.W. & Sweeney, D.W. (1975). Holographic microinterferometry of laser-produced plasmas with frequency-tripled probe pulses. *Appl. Phys. Lett*. **26**, 616–618.

Colombant, D. & Tonon, G.F. X-ray emission in laser-produced plasmas. (1973). *J. Appl. Phys*. **44**, 3524–3537.

Geohegan, D.B. (1993). Imaging and blackbody emission spectra of particulates generated in the krf-laser ablation of bn and $YBa_2Cu_3O_{7-x}$. *Appl. Phys. Lett*. **62**, 1463–1465.

Hecker-Denschlag, J., Simsarian, J.E., Ha ner, H., McKenzie, C., Browaeys, A., Cho, D., Helmerson, K., Rolston, S.L. & Phillips, W.D. (2002). A Bose-Einstein condensate in an optical lattice. *J. Phys. B: At. Mol. Opt. Phys*. **35**, 3095–3110.

Hill, W.T., Cheng, K.T., Johnson, W.R., Lucatorto, T.B., McIlrath T.J. & Sugar, J. (1982). Influence of increasing nuclear-charge on the Rydberg spectra of Xe, Cs^+, and Ba^{++}-correlation, term dependence and autoionization. *Phys. Rev. Lett*. **49**, 1631–1635.

Hirsch, J.S., Kennedy, E.T., Neogi, A., Costello, J.T., Nicolosi P. & Poletto, L. (2003). Vacuum-ultraviolet photoabsorption

imaging system for laser plasma plume diagnostics. *Rev. Sci. Instrum*. **74**, 2992–2998.

Hirsch, J.S., van Kampen, P., Meighan, O., Mosnier, J.-P., Costello, J.T., Lewis, C.L.S., MacPhee, A., Hirst, G., Westhall, J. & Shaikh, W. (2000).Vacuum-ultraviolet resonant photoabsorption imaging of laser produced plasmas. *J. Appl. Phys*. **88**, 4953–4960.

Horwitz J.L. & Moore, T.E. (2000).Core plasmas in space weather regions. *IEEE Trans. Plasma Sci*. **28**, 1840–1853.

Köble, U., Kiernan, L., Costello, J.T., Mosnier, J.-P., Kennedy, E.T., Ivanov, V.K., Kupchenko V.A. & Shendrik, M.S. (1995). 4f(^{1}P) giant-dipole resonance in La^{3+}. *Phys. Rev. Lett*. **74**, 2188–2191.

Lyon, I.C., Peart, B., West, J.B. & Dolder, K. (1987). Measurements of absolute cross sections for the photoionisation of Ba+ ions. *Journal of Physics B: Atomic and Molecular Physics* **19**, 4137–4147.

Murphy, A., Hirsch, J.S., Kilbane, D., Kennedy, E.T., Khater, M.A., Mosnier, J.-P., Neogi, A., O Sullivan, G., Lewis, C.L.S., Topping, S., Clarke, R., Divall, E., Foster, P., Hooker, C., Langley, A., Neely, D., Dunne, P. & Costello, J.T. (2003). VUV and soft x-ray emission from preplasmas irradiated with picosecond and femtosecond pulses. *Proc SPIE* **4876**, 1196–1202.

Neogi A. & Thareja, R.K. (1999). Laser-produced carbon plasma expanding in vacuum, low pressure ambient gas and nonuniform magnetic field. *Phys. Plasmas* **6**, 365–371.

Reade, R.P., Berdahl, P., Russo R.E. & Garrison, S.M. (1992). Laser deposition of biaxially textured yttria-stabilized zirconia buffer layers on polycrystalline metallic alloys for high critical current Y-Ba-Cu-O thin films. *Appl. Phys Lett*. **61**, 2231–2233.

Rose, S.J., Grant, I.P. & Connerade, J.P. (1980). A study of 5p excitation in atomic barium. *Phil. Trans. Roy. Soc. Lond*. **296**, 527.

Schulz, M., Moshammer, R., Fischer, D., Kollmus, H., Madison, D.H., Jones, S. & Ullrich, J. (2003). Three-dimensional imaging of atomic four-body processes. *Nature* **422**, 48–50.

Singh, R.K. & Narayan, J. (1990). Pulsed-laser evaporation technique for deposition of thin films: Physics and theoretical model. *Phys. Rev. B* **41**, 8843–8859.

Turcu, I.C.E., Ross, I.N., Schulz, M.S., Daido, H., Tallents, G.J., Krishnan, J., Dwivedi, L. & Hening, A. (1993). Spatial coherence measurements and x-ray holographic imaging using a laser-generated plasma x-ray source in the water window spectral region. J. Appl. Phys. **73**, 8081–8087.

Wescott, E.M., Hallinan, T.J., Steinbaeknielsen, H.C., Swift, D.W. & Wallis, D.D. (1993). Rapid ray motions in barium plasma clouds and auroras. *J. Geophys. Res*. **98**, 3711–3724.

West, J.B. (2002). Photoionization cross sections of atomic ions. *J. Elec. Spec. Radiat. Transfer* **123**, 247–256.

Williamson, T.P., Martin, G.W., El-Astal, A.H., Al-Khateeb, A., Weaver, I., Riley, D., Lamb, M.J., Morrow, T. & Lewis, C.L.S. (1999). An investigation of neutral and ion number densities within laser-produced titanium plasmas in vacuum and ambient environments. *Appl. Phys. A: Mater. Sci. Process*. **69**, S859–S863.